JACS
JOURNAL OF THE AMERICAN CHEMICAL SOCIETY
pubs.acs.org/JACS
Article

Metal and Proton Relay-Controlled Hierarchical Multistep Switching Cascade

Heyifei Fu, Susnata Pramanik, and Ivan Aprahamian*

Cite This: J. Am. Chem. Soc. 2023, 145, 19554−19560
Read Online
ACCESS | Metrics & More | Article Recommendations | Supporting Information

ABSTRACT: Transition metals play an important role in many biological processes including cellular regulation and signal transduction. Emulating such processes on the molecular level, while challenging, can help us learn how to manipulate intermolecular communication, an important requirement for the development of solution-based molecular machines. In this work, we demonstrate a transition metal-based artificial multistep switching cascade that exhibits intrinsic hierarchical level control. The process starts with Zn(II), which initiates a transition metal relay by displacing a macrocycle-encapsulated Pd(II). The latter then binds to a hydrazone switch leading to coordination-coupled deprotonation (CCD). Finally, the proton generated through CCD activates the *E*/*Z* isomerization of a second noncoordinating pH-sensitive hydrazone switch. This whole multistep process can be reset to the original state by removing the Pd(II) from the system.

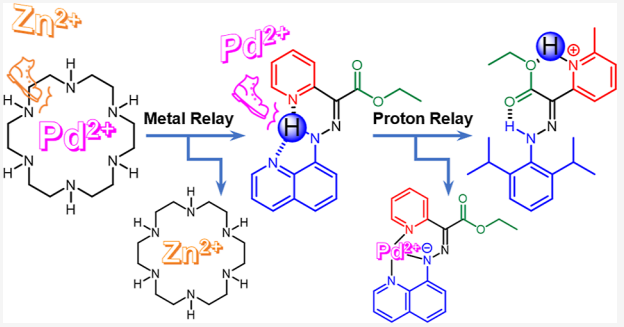

INTRODUCTION

Signal transduction is an ubiquitous form of communication in biology and is used to regulate the myriad processes necessary for life.[1] Such control usually requires multistep signal transduction events in which a cascade of reactions are triggered by a specific stimulus (e.g., multistep phosphorelay).[2,3] One of the most common strategies underlying sophisticated multistep cascades is metal exchange,[4−7] the study of which[8] has helped us understand how cell machinery select the correct transition metal to accomplish a particular goal. Zn(II) ions are privileged in this regard because they play an important role as signal transducers in cellular regulation, neurotransmission, immunology, and skin formation, among other processes, and hence, their biological activity has been extensively studied.[9−12] Inspired by the findings of these studies, we developed[13,14] a number of hydrazone switches, such as **1** (Scheme 1), that undergo coordination-coupled deprotonation (CCD) upon coordination with Zn(II).[15]

This biologically relevant[16] process and the proton relay it enables were later used by us in designing synthetic systems that exhibit intermolecular communication,[17] catalysis-based amplification,[18] and negative feedback loop function.[19] These examples of intermolecular communication are some of the most complicated, molecular switch-based[20,21] synthetic reaction cascades reported, which have recently been supplemented by systems where a combination of metal redox, exchange, and relay are used to communicate between up to three species.[22−24] These latter systems, while beautiful, rely on well-established, and sometimes structurally intricate, metal coordination motifs.[25−29] Considering the importance of metal exchange and relays (including of protons) in biological systems and the limited structural space of synthetic systems that can mimic such processes, there is a critical need to explore and develop alternative systems that can accomplish similar goals. Here, we report on a hydrazone-based hierarchical multistep switching cascade that combines metal exchange and CCD-induced proton relay (Figure 1). Initially, the macrocyclic ligand **2** encapsulates and compartmentalizes Pd(II) ions, so they will not interact with the hydrazone

Scheme 1. Switching via Coordination-Coupled Proton Transfer in 1

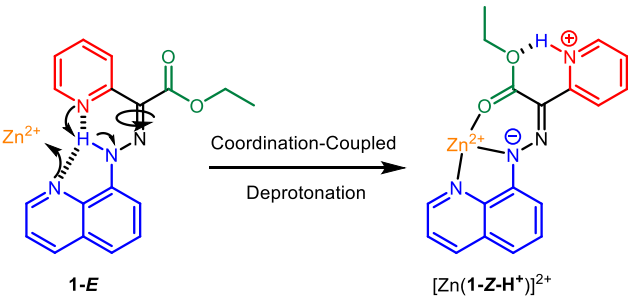

Received: March 21, 2023
Published: August 29, 2023

https://doi.org/10.1021/jacs.3c02855
J. Am. Chem. Soc. 2023, 145, 19554−19560

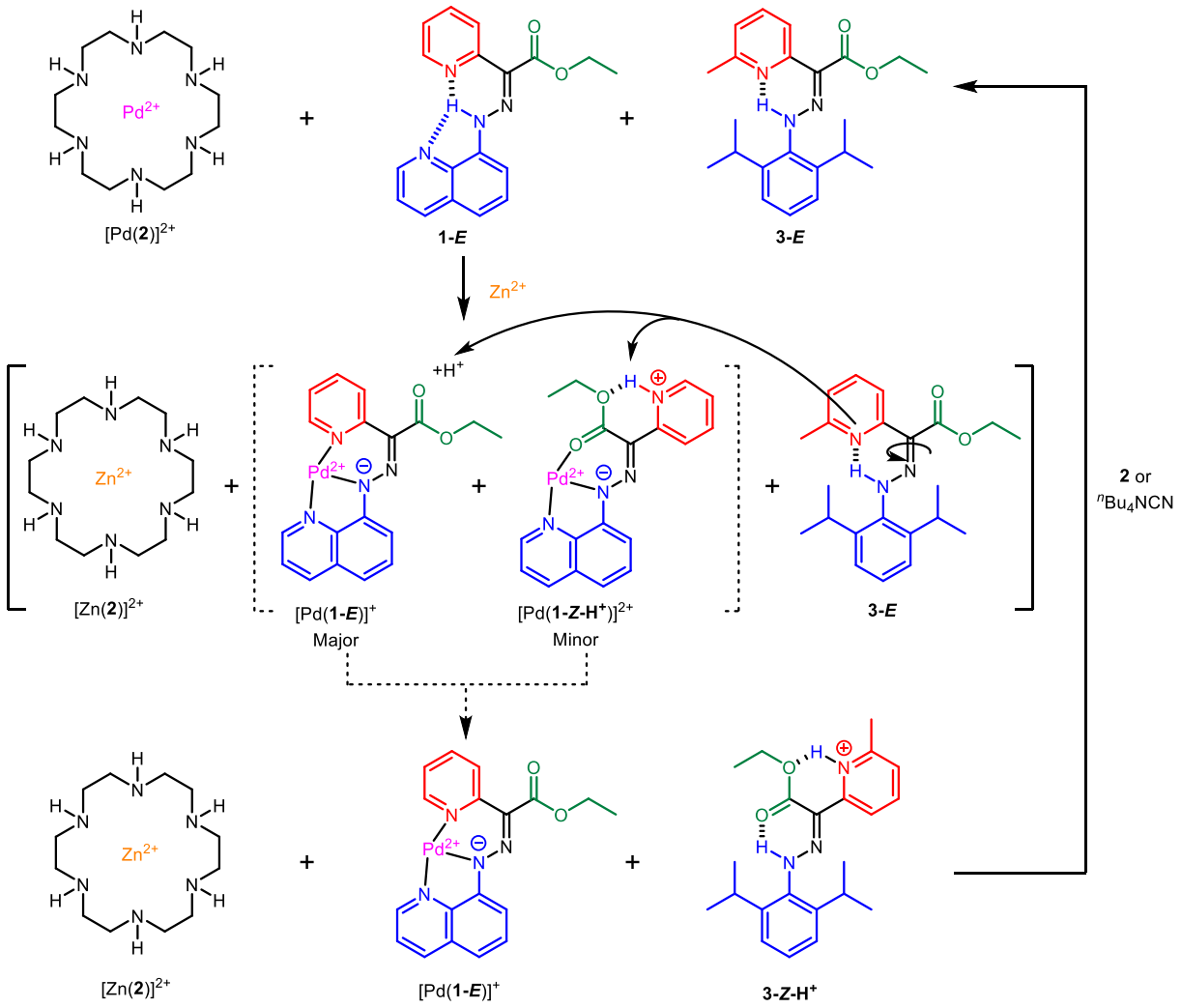

Figure 1. Reversible hierarchical multistep switching cascade that relies on transition metal and proton relays. The addition of Zn(II) to a solution of $[Pd(\mathbf{2})]^{2+}$, **1**-*E* and **3**-*E* initiates a transition metal relay from $[Pd(\mathbf{2})]^{2+}$ to **1**-*E*. The Pd(II) triggers a CCD process with **1**-*E*, followed by a proton relay that results in **3**-*Z*-H^+.

switches **1** and **3**. When Zn(II) is added to the solution, it displaces Pd(II) from the macrocyclic complex, which coordinates to **1**-*E*, yielding either $[Pd(\mathbf{1}\text{-}Z\text{-}H^+)]^{2+}$ or $[Pd(\mathbf{1}\text{-}E)]^+$. Subsequently, a proton relay from the latter triggers the configurational change of a noncoordinated hydrazone **3**. This whole process can be reversed by i) removing the Pd(II) from hydrazone **1** using extra ligand **2** or ii) completely removing all the metal cations using an excess amount of cyanide. This work is a proof of principle showing that sophisticated signal transduction pathways can be realized using transition metal ions (including a biologically relevant one) and simple hydrazone switches. Such studies can in the future provide insights into how biological systems design and manipulate metal- and proton-based signaling pathways.[9−12]

RESULTS AND DISCUSSION

Synthesis. Known hydrazone switches **1** and **4** were synthesized according to reported procedures.[30,31] Hydrazone switches **3**, **5**, and **6** were synthesized using a facile one-pot procedure starting from appropriately substituted anilines and ethyl-2-pyridyl acetate derivatives in 24−51% yield. The *E* isomers of the hydrazones were separated as the major products in all reactions. The assignment of the *E* isomer was corroborated by the downfield chemical shift of the hydrazone NH proton (14.28−14.68 ppm), arising from its intramolecular H-bond with the pyridyl nitrogen. All the hydrazones were characterized using NMR spectroscopy and mass spectrometry (see the Supporting Information for synthetic details and characterization).

After screening a number of potential hydrazone candidates (See SI for details, Figures S17−S29), switches **1** and **4** (Scheme 2a) were selected as the candidates for the development of the hitherto unexplored Pd(II)-initiated CCD process (*vide infra*). Meanwhile, the newly designed hydrazones **3**, **5**, and **6** (Scheme 2b) were chosen as the noncoordinating acid-responsive switch candidates (for the other hydrazones that were screened but not discussed here, please see Section S5 of the Supporting Information).

Coordination Studies. First, we set out to identify a host ligand that can initially act as a reservoir to either Pd(II) or Zn(II) (i.e., have a lower affinity to one of the metal ions), which can subsequently be released upon binding with the metal having the stronger affinity. We decided to go with macrocycle **2** as it is known to bind many transition metals[32] and, more importantly, because of its reported preference (i.e., 10 orders of magnitude stronger binding) to Pd(II) over

https://doi.org/10.1021/jacs.3c02855
J. Am. Chem. Soc. 2023, 145, 19554−19560

Scheme 2. (a) Hydrazone Switches Studied for the Development of Pd(II)-Initiated CCD Process. (b) Hydrazone switches studied as the proton acceptors in the relay process

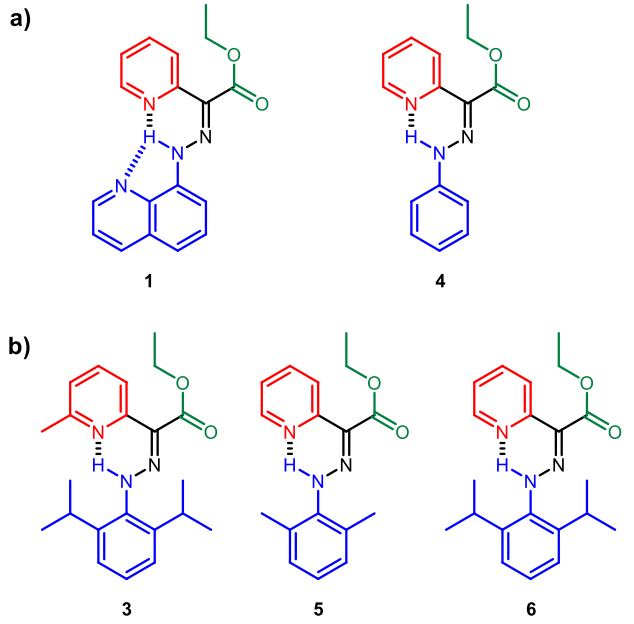

[a](b) Hydrazone switches studied as the proton acceptors in the relay process.

Zn(II) in water.[32,33] Based on these studies Pd(II) forms 1:1 and 2:1 complexes with **2**, with binding constants of $K_1 = 1.6 \times 10^{29}$ M^{-1} ($[Pd(\mathbf{2})]^{2+}$) and $K_2 = 6.3 \times 10^{51}$ M^{-1} ($[Pd_2(\mathbf{2})Cl_2]^{2+}$), while Zn(II) only forms a 1:1 complex under similar conditions with a binding constant of $K = 5.0 \times 10^{18}$ M^{-1} ($[Zn(\mathbf{2})]^{2+}$). Surprisingly, ^{1}H NMR spectroscopy studies showed that the relative binding affinities of Pd(II) and Zn(II) to **2** were reversed in CD_3CN compared to water (Figure S15). To further elaborate on this trend, isothermal titration calorimetry (ITC) was employed to study the binding affinity between **2** and the transition metal cations (Table 1). The ITC

Table 1. Binding Constants Measured Using ITC (25 °C in CH_3CN)

complexation	K_1 (M^{-1})	K_2 (M^{-1})
$[Zn(\mathbf{2})]^{2+}$[a]	$1.47 \pm 0.38 \times 10^{14}$	
$[Pd(\mathbf{2})]^{2+}$	$7.23 \pm 0.24 \times 10^{8}$	$2.29 \pm 0.22 \times 10^{6}$
$[Pd(\mathbf{1})]^{+}$	$1.06 \pm 0.08 \times 10^{6}$	
$[Pd(\mathbf{4})]^{+}$	$2.33 \pm 0.90 \times 10^{7}$	$1.19 \pm 0.10 \times 10^{6}$

[a]The binding constant of $[Zn(\mathbf{2})]^{2+}$ was obtained by the competitive binding experiment of $Zn(ClO_4)_2$ and $[Pd(\mathbf{2})]^{2+}$.

measurements showed a 2:1 binding between Pd(II) and **2** (Figure S46), with binding constants of $K_1 = 7.23 \times 10^8$ M^{-1} and $K_2 = 2.29 \times 10^6$ M^{-1}. Competitive binding experiments were then used to obtain the binding constant of Zn(II) with **2** because the value exceeded the upper detection limit of the ITC instrument. The binding constant was calculated to be 1.47×10^{14} M^{-1} (Figure S45), which is 6 orders of magnitude larger than that of Pd(II) in CH_3CN.

The binding stoichiometry was further supported by X-ray analysis of single crystals of $[Zn(\mathbf{2})](ClO_4)_2$, $[Pd(\mathbf{2})](BF_4)_2$, and $[Pd_2(\mathbf{2})(CH_3CN)_2](BF_4)_4$. In the 1:1 complex of $[Zn(\mathbf{2})]^{2+}$ (Figure 2a), the Zn(II) cation is hexacoordinated with **2** (Zn−N, 2.180(5)-2.251(4) Å) and adopts an

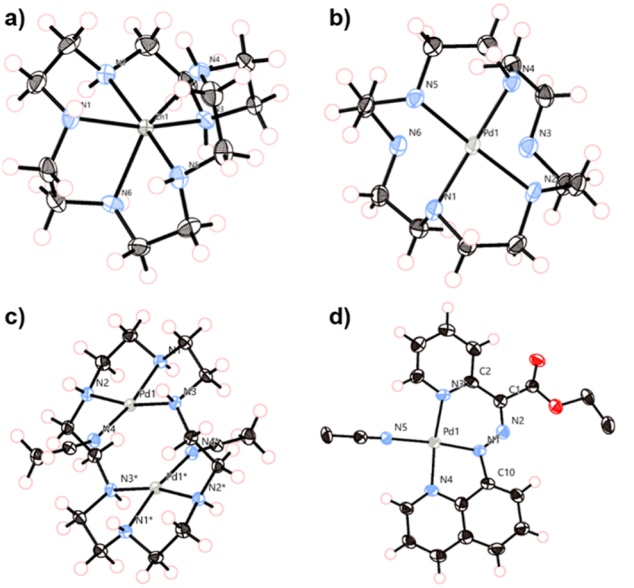

Figure 2. ORTEP drawing (50% probability ellipsoids) of the X-ray crystal structures of (a) $[Zn(\mathbf{2})](ClO_4)_2$; (b) $[Pd(\mathbf{2})](BF_4)_2$; (c) $[Pd_2(\mathbf{2})(CH_3CN)_2](BF_4)_4$; and (d) $[Pd(\mathbf{1})(CH_3CN)]BF_4$. The anions are omitted for the sake of clarity.

octahedral geometry. In both the 1:1 and 2:1 complexes of Pd(II) and **2** (Figure 2b,c), the Pd(II) cation is tetracoordinated with **2** and adopts a square planar geometry. In the case of $[Pd(\mathbf{2})](BF_4)_2$, the distance of Pd···N3 (2.951(4) Å) and Pd···N6 (2.885(4) Å) are longer than the other Pd−N bonds (2.047(4)-2.113(3) Å), which implies that only four nitrogen atoms participate in the coordination. In the 2:1 complex, all the Pd−N bond distances are similar (2.007(2)-2.065(3) Å) and the Pd···Pd distance is 3.0311(4) Å.

Pd(II)-Initiated CCD. To expand the reach of CCD into more sophisticated adaptive functional systems, we set up to develop a new Pd(II)-initiated CCD process. After some initial screening (see Supporting Information for more details), we focused on hydrazones **1** and **4** as possible targets for accomplishing this goal. The binding of Pd(II) with **1** and **4** was studied by ITC (Table 1), and ^{1}H NMR and UV/vis spectroscopies. The ITC studies indicated a 1:1 binding stoichiometry for the complexation of Pd(II) with **1** and a binding constant of 1.06×10^6 M^{-1} (Figure S47). The stoichiometry was also corroborated using a Job's plot analysis (Figure S49). Fortunately, the binding constant measured for Pd(II) and hydrazone **1** was in the correct range (i.e., lower than **2**) to enable the hierarchical sequence required for the multistep switching cascade. In contrast, the ITC titration results with **4** yielded two binding events with equilibria constants of $K_1 = 2.33 \times 10^7$ M^{-1} and $K_2 = 1.19 \times 10^6$ M^{-1} (Figure S48). These results show that **4** would compete with **2** on the coordination of Pd(II), and so, we decided to use hydrazone **1** in our subsequent switching cascade studies.

The ^{1}H NMR spectrum of **1-*E*** changes drastically after the addition of Pd(II) (1.0 equiv) to the solution (Figure 3b). For example, the hydrazone N−H proton signal of **1-*E*** (δ = 15.38 ppm) disappears, indicating coordination with Pd(II). In general, the aromatic signals of **1-*E*** are shifted downfield upon

https://doi.org/10.1021/jacs.3c02855
J. Am. Chem. Soc. 2023, 145, 19554−19560

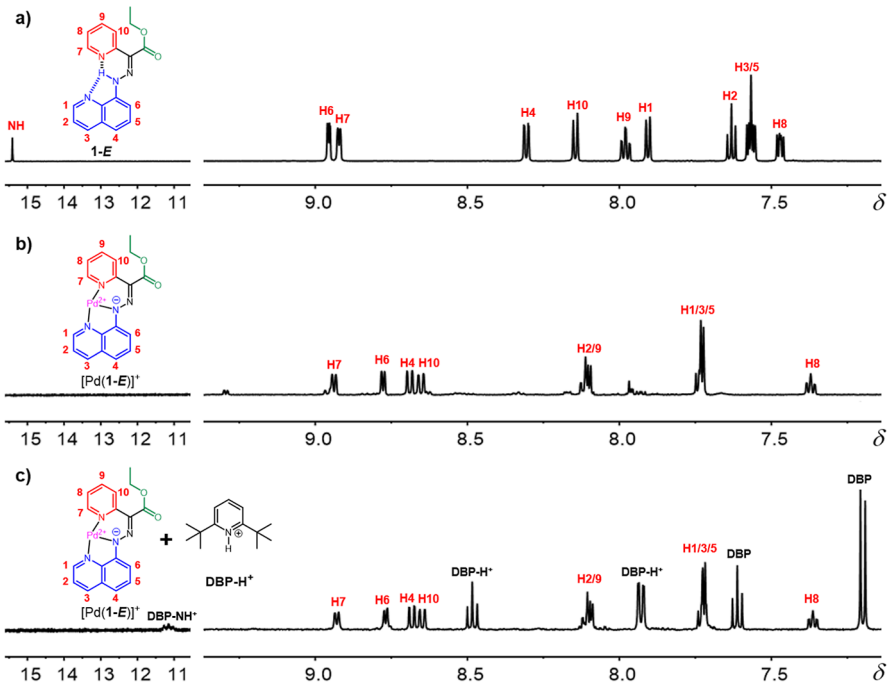

Figure 3. ^{1}H NMR spectra (CD_3CN, 298 K) of (a) **1-*E***; (b) [Pd(**1-*E***)]$^+$ recorded after mixing an equimolar amount of Pd(II) and **1** ([**1**] = 1.3 mM); and (c) [Pd(**1-*E***)]$^+$ and protonated 2,6-di-*tert*-butylpyridine (**DPB-H**$^+$) recorded after mixing an equimolar amount of Pd(II), **1-*E***, and **DPB** ([**1**] = 1.3 mM).

complexation, except for protons H1, H6, and H8. A similar trend was observed upon protonation of the pyridyl ring in **1**, indicating the development of a positive charge on the ring.[30,34] However, unlike what is observed in general with Zn(II) where CCD triggers an *E*/*Z* isomerization and results in a Zn(II)-bound protonated complex (Scheme 1),[15,17] the signal of the protonated pyridinium was not observed with Pd(II) (Figure 3b). To confirm the occurrence of Pd(II)-induced CCD, we conducted a control experiment using 2,6-di-*tert*-butylpyridine (**DBP**) as a noncoordinated proton acceptor. The addition of 1.0 equiv of Pd(II) to an equimolar mixture of **1-*E*** and **DBP** (Figure 3c) resulted in the appearance of signals of protonated **DBP** (**DPB-H**$^+$), indicating that the coordination of Pd(II) led to the deprotonation of **1-*E*** and the release of protons to the solution. The fact that the chemical shifts of Pd(II)-bound **1** were almost the same in the presence and absence of the base (i.e., the chemical shift of the pyridyl ring is not shifting) made us speculate that Pd(II) is bound to the pyridyl nitrogen instead of the carbonyl oxygen, i.e., coordination might not result in $E \rightarrow Z$ isomerization in this case. We observed a similar outcome with Zn(II) as well in systems where the pyridyl ring was replaced with an imidazolyl one.[18] This assignment of [Pd(**1-*E***)]$^+$ was confirmed using X-ray analysis studies (Figure 2d). In the 1:1 complex between Pd(II) and **1**, the hydrazone has a planar geometry, while the Pd(II) cation is tetracoordinated (with three nitrogen atoms from **1** and one acetonitrile molecule). The ^{1}H NMR spectrum obtained after dissolving crystals used in the X-ray analysis in CD_3CN showed identical signals to [Pd(**1-*E***)]$^+$ (Figure S30e). These results show that the final outcome of the coordination of **1** with Pd(II) results in a complex that retains the original configuration of the hydrazone. We also performed Pd(II) binding studies with **4** and similar results were obtained (Figures S32 and S33).

Interestingly, the ^{1}H NMR spectrum obtained right after mixing an equimolar amount of Pd(II), **1-*E***, and **DBP** (Figure S34) shows another small set of signals belonging to a Pd(II)-bound **1** species. Correlation spectroscopy (COSY, Figure S35) analysis indicated that this new set of signals corresponds to [Pd(**1-*Z***)]$^+$ (Figure 1). In the absence of the base (Figure S30f) a broad signal at δ = 13.37 ppm can be observed in the ^{1}H NMR spectrum when acquired at a low temperature (238 K). This signal is similar in shape and chemical shift to the protonated pyridinium N$^+$−H proton signal observed in Zn(II)-triggered CCD.[15] The broadness and low intensity of this signal, however, precluded the observation of any COSY interactions with it. The fact that these minor signals diminish in intensity after seven days indicates that this is a kinetic product, which converts to the thermodynamically stable one with time, i.e., [Pd(**1-*Z***)]$^+$ converts to [Pd(**1-*E***)]$^+$.

Proton Acceptor. Next, to achieve the last step of the cascade, we set out to identify an acid-responsive hydrazone switch that does not bind to either Zn(II) or Pd(II). Given the previous observation that **4** does not coordinate to Zn(II),[17] three different hydrazones (**3**, **5**, and **6**) were designed based on its core (Scheme 2b). The Pd(II)-induced proton relay process was then studied by ^{1}H NMR spectroscopy using equimolar mixtures of Pd(II), **1**, and the respective acid-responsive hydrazone. Mixing of Pd(II), **1**, and **5** showed that 37% of **5** was coordinated to Pd(II), whereas 63% was protonated (Figure S27). Hydrazone **6** which has an isopropyl group on its phenyl group instead of a methyl one, as is the case in **5**, results in an improved coordination/protonation ratio of 25:75%, respectively (Figure S28). Finally, substituting the pyridyl ring as well with a methyl group at the *ortho* position (**3**) completely blocks binding to Pd(II) and results in 100% protonation (Figure S26). Based on these results, **3** was chosen as the noncoordinated acid-responsive hydrazone switch for realizing the switching cascade.

https://doi.org/10.1021/jacs.3c02855
J. Am. Chem. Soc. 2023, 145, 19554−19560

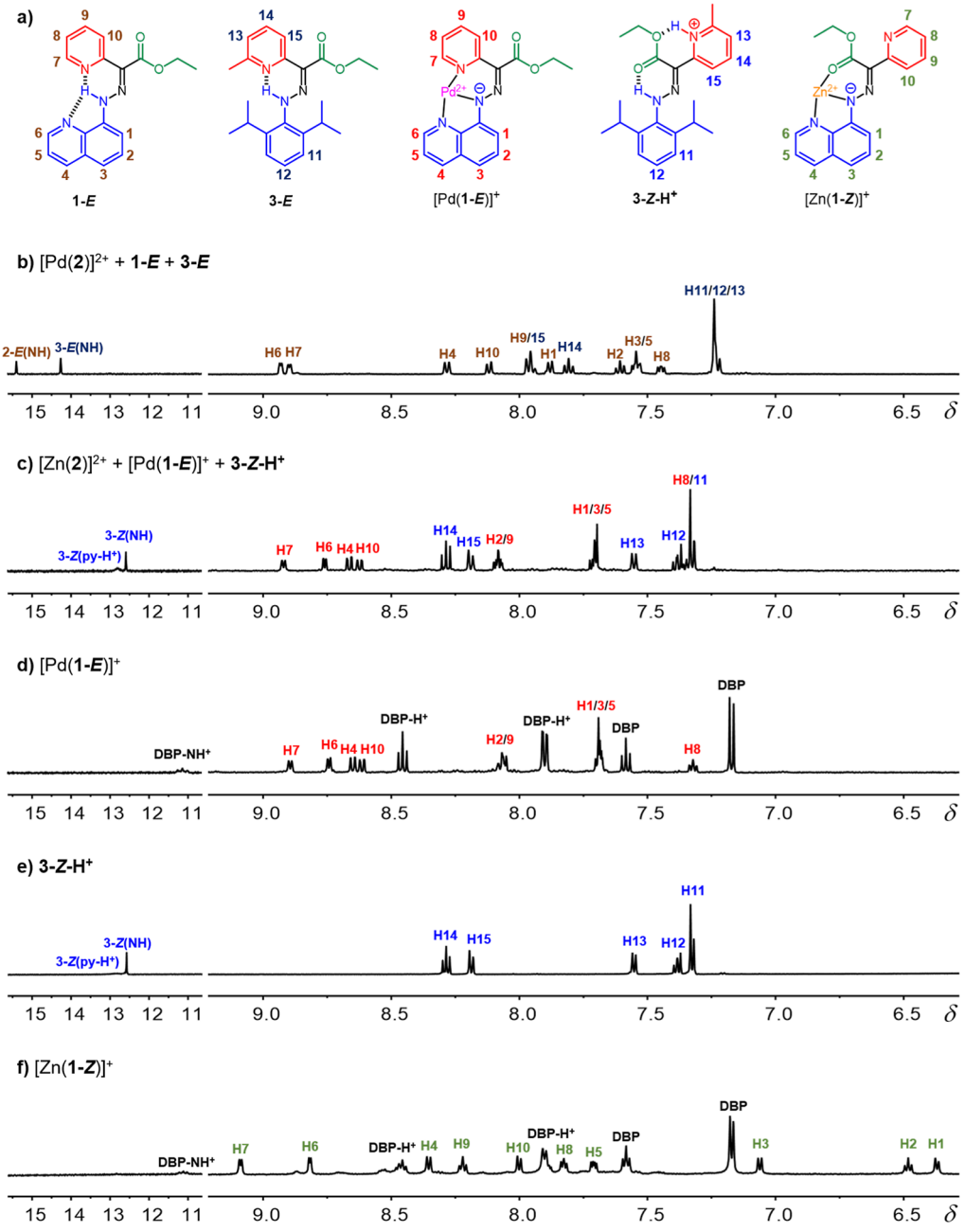

Figure 4. Multi-input switching cascade. (a) Structures of different hydrazones used in the studies; (b) ^{1}H NMR spectra (CD_3CN, 298 K) of $[Pd(\mathbf{2})]^{2+}$ (Pd(II) 1.4 equiv), **1**-*E*, and **3**-*E* (initial state, equimolar of **1**-*E*, **2** and **3**-*E*, [**1**] = 1.3 mM); (c) $[Zn(\mathbf{2})]^{2+}$, $[Pd(\mathbf{1}\text{-}E)]^+$, and **3**-*Z*-$H^+$ (final state) obtained after the addition of 1.0 equiv Zn(II); (d) $[Pd(\mathbf{1}\text{-}E)]^+$ obtained by mixing equimolar amounts of Pd(II), **1**, and **DBP** ([**1**] = 1.3 mM); (e) **3**-*Z*-H^+ obtained by adding an excess amount of trifluoroacetic acid (**TFA**) into **3**; and (f) $[Zn(\mathbf{1}\text{-}Z)]^+$ obtained by mixing equimolar amounts of Zn(II), **1**, and **DBP** ([**1**] = 1.3 mM).

Hierarchical Multistep Switching Cascade. After identifying the appropriate pieces of the puzzle, we set out to study the multistep switching cascade involving a transition metal relay coupled to a proton relay using ^{1}H NMR spectroscopy. To determine the maximum amount of Pd(II) that can be encapsulated by **2** under the switching cascade conditions, equimolar mixtures of **1**, **2**, and **DBP** were prepared, and 1.0−1.4 equiv of Pd(II) was gradually titrated into the solution (Figure S36). The signals of **1** remained unchanged up to 1.4 equiv of Pd(II), and no protonated **DBP** signals were observed at this stage. Using **3** instead of **DBP** resulted in the same outcome (Figure S38). These observations imply that **2** can encapsulate up to 1.4 equiv of Pd(II) in the presence of **1** without significant amount of metal ion "leakage".

Finally, the feasibility of the switching cascade was studied (Figure 4). After mixing **2** (1.0 equiv), Pd(II) (1.4 equiv), **1** (1.0 equiv), and **3** (1.0 equiv) together, the ^{1}H NMR spectrum showed signals belonging to **1** and **3** in the aromatic region, whereas the signals of protonated or metal-coordinated hydrazones were absent, as expected (Figure 4b). After the addition of Zn(II) (1.0 equiv) to the solution, it became encapsulated by **2** and the metal ion relay of Pd(II) from **2** to **1** occurred. The subsequent Pd(II)-induced CCD process led to

https://doi.org/10.1021/jacs.3c02855
J. Am. Chem. Soc. 2023, 145, 19554−19560

proton relay, leading to the protonation of the acid-responsive hydrazone **3** (Figure 4c). Accordingly, the N−H proton signal of **1**-***E*** at δ = 15.38 ppm disappeared completely, indicating that the CCD process reached completion. The N−H proton signal of **3**-***E***, which was originally at 14.25 ppm, underwent an upfield shift to 12.58 ppm, indicating that the *o*-methyl-pyridyl ring in hydrazone **3** was protonated.[30] The proton signals belonging to **3**-***Z***-$\mathbf{H}^+$ at δ = 8.29, 8.19, 7.55, 7.38, and 7.33 ppm (Figure 4e) all shift to a lower field compared with the initial **3**-***E*** signals because of protonation, which also implies that the proton relay occurred. None of the characteristic proton signals (i.e., H3, H2, and H1 at δ = 7.06, 6.48, and 6.37 ppm) belonging to $[Zn(\mathbf{1}\text{-}\mathbf{Z})]^+$ (Figure 4f) could be detected in the final state of the switching cascade, while all the signals belonging to $[Pd(\mathbf{1}\text{-}\mathbf{E})]^+$ (Figure 4d) are observed. These findings clearly indicate that Zn(II) was fully encapsulated by **2** and did not participate in the CCD process, while Pd(II) was involved in a metal relay and subsequent activation of the CCD.

After the switching cascade reached completion, we reset the whole system to its initial state in two different ways (Figure S41): i) addition of $^n\mathrm{Bu}_4\mathrm{NCN}$ [12.0 equiv relative to existing hydrazone **1**, overall 5.0 equiv relative to the total amount of Pd(II) and Zn(II)] to the final mixture, which removed the Pd(II) and Zn(II) from **1** and **2**, respectively, reverting the two switches, **1** and **3**, to their original state (Figure S41d) and ii) addition of surplus **2** (1.5 equiv relative to existing hydrazone **1**) to the final mixture which removed the metal from $[Pd(\mathbf{1}\text{-}\mathbf{E})]^+$, reverting **1** and **3** back to their original state (Figure S41e) and resulting in $[Pd(\mathbf{2})]^{2+}$ (Figure S42). Addition of another batch of Zn(II) (1.25 equiv relative to existing hydrazone **1**) to the reset system starts the whole cascade event again (Figure S43).

CONCLUSIONS

We have successfully developed a three-component molecular system that can communicate with each other via coupled transition metal and proton relays. After much optimization, macrocycle **2** was incorporated into a Zn(II)-triggered three-step switching cascade which includes the Zn(II)-induced relay of Pd(II) from **2** to **1**, followed by a proton relay from $[Pd(\mathbf{1}\text{-}\mathbf{E})]^+$ to the acid-responsive switch **3**. This proof-of-principle demonstration, which is one of the most complicated switching cascades developed so far, showcases how intermolecular communication can be realized by judiciously combining appropriate transition metals and hydrazone switches together. On top of showing how fine-tuned such processes are, these results also provide insights into how to artificially mimic biologically relevant signal transduction cascades[4−7,9−12] using simplified metal and pH-responsive building blocks.

ASSOCIATED CONTENT

Supporting Information

The Supporting Information is available free of charge at https://pubs.acs.org/doi/10.1021/jacs.3c02855.

General methods, experimental procedures, NMR spectra of key compounds, ITC and crystal data for $[Zn(\mathbf{2})](ClO_4)_2$, $[Pd(\mathbf{2})](BF_4)_2$, $[Pd_2(\mathbf{2})(CH_3CN)_2](BF_4)_4$, and $[Pd(\mathbf{1})(CH_3CN)]BF_4$ (PDF)

Accession Codes

CCDC 2162419−2162422 contain the supplementary crystallographic data for this paper. These data can be obtained free of charge via www.ccdc.cam.ac.uk/data_request/cif, or by emailing data_request@ccdc.cam.ac.uk, or by contacting The Cambridge Crystallographic Data Centre, 12 Union Road, Cambridge CB2 1EZ, UK; fax: +44 1223 336033.

AUTHOR INFORMATION

Corresponding Author

Ivan Aprahamian − *6128 Burke Laboratory, Department of Chemistry, Dartmouth College, Hanover, New Hampshire 03755, United States;* orcid.org/0000-0003-2399-8208; Email: ivan.aprahamian@dartmouth.edu

Authors

Heyifei Fu − *6128 Burke Laboratory, Department of Chemistry, Dartmouth College, Hanover, New Hampshire 03755, United States*

Susnata Pramanik − *6128 Burke Laboratory, Department of Chemistry, Dartmouth College, Hanover, New Hampshire 03755, United States; Department of Chemistry, SRM Institute of Science and Technology, Kattankulathur 603203, India*

Complete contact information is available at: https://pubs.acs.org/10.1021/jacs.3c02855

Notes

The authors declare no competing financial interest.

ACKNOWLEDGMENTS

This work was supported by the NSF MSN program (CHE-2304983). We gratefully acknowledge Prof. Richard Staples (Michigan State University) for the X-ray data.

REFERENCES

(1) Chen, R. E.; Thorner, J. Systems Biology Approaches in Cell Signaling Research. *Genome Biol.* **2005**, *6*, 235.

(2) Burbulys, D.; Trach, K. A.; Hoch, J. A. Initiation of Sporulation in B. Subtilis Is Controlled by a Multicomponent Phosphorelay. *Cell* **1991**, *64*, 545−552.

(3) Appleby, J. L.; Parkinson, J. S.; Bourret, R. B. Signal Transduction via the Multi-Step Phosphorelay: Not Necessarily a Road Less Traveled. *Cell* **1996**, *86*, 845−848.

(4) Moulis, J.-M. Cellular Dynamics of Transition Metal Exchange on Proteins: A Challenge but a Bonanza for Coordination Chemistry. *Biomolecules* **2020**, *10*, 1584.

(5) Wösten, M. M. S. M.; Kox, L. F. F.; Chamnongpol, S.; Soncini, F. C.; Groisman, E. A. A Signal Transduction System That Responds to Extracellular Iron. *Cell* **2000**, *103*, 113−125.

(6) Maret, W. Zinc Biochemistry: From a Single Zinc Enzyme to a Key Element of Life. *Adv. Nutr.* **2013**, *4*, 82−91.

(7) Grubman, A.; White, A. R. Copper as a Key Regulator of Cell Signalling Pathways. *Expert Rev. Mol. Med.* **2014**, *16*, No. e11.

(8) Dudev, T.; Lim, C. Competition among Metal Ions for Protein Binding Sites: Determinants of Metal Ion Selectivity in Proteins. *Chem. Rev.* **2014**, *114*, 538−556.

(9) Fukada, T.; Kambe, T. *Zinc Signaling*; Springer: Singapore, 2019.

(10) Maywald, M.; Wessels, I.; Rink, L. Zinc Signals and Immunity. *Int. J. Mol. Sci.* **2017**, *18*, 2222.

(11) Subramanian Vignesh, K.; Deepe Jr, G. Metallothioneins: Emerging Modulators in Immunity and Infection. *Int. J. Mol. Sci.* **2017**, *18*, 2197.

(12) Maret, W. Zinc in Cellular Regulation: The Nature and Significance of "Zinc Signals. *Int. J. Mol. Sci.* **2017**, *18*, 2285.

(13) Shao, B.; Aprahamian, I. Hydrazones as New Molecular Tools. *Chem* **2020**, *6*, 2162−2173.

(14) Aprahamian, I. Hydrazone Switches and Things in Between. *Chem. Commun.* **2017**, *53*, 6674−6684.
(15) Su, X.; Robbins, T. F.; Aprahamian, I. Switching through Coordination-Coupled Proton Transfer. *Angew. Chem., Int. Ed.* **2011**, *50*, 1841−1844.
(16) Williams, R. J. P. Proton Circuits in Biological Energy Interconversions. *Annu. Rev. Biophys. Biophys. Chem.* **1988**, *17*, 71−97.
(17) Ray, D.; Foy, J. T.; Hughes, R. P.; Aprahamian, I. A Switching Cascade of Hydrazone-Based Rotary Switches through Coordination-Coupled Proton Relays. *Nat. Chem.* **2012**, *4*, 757−762.
(18) Foy, J. T.; Ray, D.; Aprahamian, I. Regulating Signal Enhancement with Coordination-Coupled Deprotonation of a Hydrazone Switch. *Chem. Sci.* **2015**, *6*, 209−213.
(19) Pramanik, S.; Aprahamian, I. Hydrazone Switch-Based Negative Feedback Loop. *J. Am. Chem. Soc.* **2016**, *138*, 15142−15145.
(20) Harris, J. D.; Moran, M. J.; Aprahamian, I. New Molecular Switch Architectures. *Proc. Natl. Acad. Sci. U.S.A.* **2018**, *115*, 9414−9422.
(21) Our focus here is on systems that exhibit molecular motion upon interacting with a stimulus, i.e., molecular switches. Lehn and co-workers have extensively described systems that undergo constitutional dynamic library switching upon multi-metal coordination cascades. For representative examples, please see: (a) Ulrich, S.; Lehn, J.-M. Adaptation to Shape Switching by Component Selection in a Constitutional Dynamic System. *J. Am. Chem. Soc.* **2009**, *131*, 5546−5559. (b) He, M.; Lehn, J.-M. Time-Dependent Switching of Constitutional Dynamic Libraries and Networks from Kinetic to Thermodynamic Distributions. *J. Am. Chem. Soc.* **2019**, *141*, 18560−18569. (c) He, M.; Lehn, J.-M. Metal Cation-Driven Dynamic Covalent Formation of Imine and Hydrazone Ligands Displaying Synergistic Co-catalysis and Auxiliary Amine Effects. *Chem.—Eur. J.* **2021**, *27*, 7516−7524. (d) Osypenko, A.; Cabot, R.; Armao, J. J.; Kovaříček, P.; Santoro, A.; Lehn, J.-M. Behavior of Constitutional Dynamic Networks: Competition, Selection, Self-sorting in Cryptate Systems. *ChemistryEurope* **2023**, *1*, No. e202300017.
(22) Schmittel, M. Networking Switches for Smart Functions Using Copper Signaling and Dynamic Heteroleptic Complexation. *Dalton Trans.* **2018**, *47*, 6654−6659.
(23) Pramanik, S.; De, S.; Schmittel, M. Bidirectional chemical communication between nanomechanical switches. *Angew. Chem., Int. Ed.* **2014**, *53*, 4709−4713.
(24) Pramanik, S.; De, S.; Schmittel, M. A Trio of Nanoswitches in Redox-Potential Controlled Communication. *Chem. Commun.* **2014**, *50*, 13254−13257.
(25) Constable, E. D.; Housecroft, C. E. The Early Years of 2,2'-Bipyridine—A Ligand in Its Own Lifetime. *Molecules* **2019**, *24*, 3951.
(26) Rashid, S.; Yoshigoe, Y.; Saito, S. Phenanthroline Based Rotaxanes: Recent Developments in Syntheses and Applications. *RSC Adv.* **2022**, *12*, 11318−11344.
(27) Bencini, A.; Lippolis, V. 1,10-Phenanthroline: A Versatile Building Block for the Construction of Ligands for Various Purposes. *Coord. Chem. Rev.* **2010**, *254*, 2096−2180.
(28) Wei, C.; He, Y.; Shi, X.; Song, Z. Terpyridine-Metal Complexes: Applications in Catalysis and Supramolecular Chemistry. *Coord. Chem. Rev.* **2019**, *385*, 1−19.
(29) Shi, J.; Wang, M. Self-Assembly Methods for Recently Reported Discrete Supramolecular Structures Based on Terpyridine. *Chem.—Asian J.* **2021**, *16*, 4037−4048.
(30) Landge, S. M.; Tkatchouk, E.; Benítez, D.; Lanfranchi, D. A.; Elhabiri, M.; Goddard, W. A.; Aprahamian, I. Isomerization Mechanism in Hydrazone-Based Rotary Switches: Lateral Shift, Rotation, or Tautomerization? *J. Am. Chem. Soc.* **2011**, *133*, 9812−9823.
(31) Su, X.; Lõkov, M.; Kütt, A.; Leito, I.; Aprahamian, I. Unusual Para-Substituent Effects on the Intramolecular Hydrogen-Bond in Hydrazone-Based Switches. *Chem. Commun.* **2012**, *48*, 10490−10492.
(32) Bianchi, A.; Micheloni, M.; Paoletti, P. Thermodynamic Aspects of the Polyazacycloalkane Complexes with Cations and Anions. *Coord. Chem. Rev.* **1991**, *110*, 17−113.
(33) Bazzicalupi, C.; Bencini, A.; Bianchi, A.; Giorgi, C.; Valtancoli, B. Pd(II) Complexes of Aliphatic Polyamine Ligands in Aqueous Solution: Thermodynamic and Structural Features. *Coord. Chem. Rev.* **1999**, *184*, 243−270.
(34) Su, X.; Aprahamian, I. Switching Around Two Axles: Controlling the Configuration and Conformation of a Hydrazone-Based Switch. *Org. Lett.* **2011**, *13*, 30−33.

https://doi.org/10.1021/jacs.3c02855
J. Am. Chem. Soc. 2023, 145, 19554−19560